PHYSICAL REVIEW D **94,** 054018 (2016)

# Searches for top-Higgs FCNC couplings via the $Whj$ signal with $h \to \gamma\gamma$ at the LHC

Yao-Bei Liu[1,*] and Zhen-Jun Xiao[2,†]

[1]*Henan Institute of Science and Technology, Xinxiang 453003, People's Republic of China*
[2]*Department of Physics and Institute of Theoretical Physics, Nanjing Normal University, Nanjing 210023, People's Republic of China*

(Received 4 May 2016; published 16 September 2016)

In this paper, we investigated the process $pp \to W^- hj$ induced by the top-Higgs flavor-changing neutral current couplings at the LHC. We found that the cross section of $pp \to W^- hj$ mainly comes from the resonant process $pp \to W^- t \to W^- hq$ due to the anomalous $tqH$ couplings (where $q$ denotes up and charm quarks). We further studied the observability of the top-Higgs flavor-changing neutral current couplings through the process $pp \to W^-(\to \ell^- \bar{\nu}_\ell) h(\to \gamma\gamma) j$ and found that the branching ratios $\mathrm{Br}(t \to qh)$ can be probed to 0.16% at $3\sigma$ level at 14 TeV LHC with an integrated luminosity of 3000 $\mathrm{fb}^{-1}$.

DOI: 10.1103/PhysRevD.94.054018

## I. INTRODUCTION

The discovery of a 125 GeV Higgs boson at CERN's LHC Run I [1,2] has heralded the beginning of a new era of Higgs physics. So far, the observed signal strengths, albeit with large experimental uncertainties, are found to be in good agreement with the predictions of the Standard Model (SM) [3,4]. Thus, precise measurements of Higgs boson couplings to the SM particles will be a dominant task at the LHC in the next decades.

The top quark, the heaviest element of the SM, owns the largest Yukawa coupling to the Higgs boson and has the preference to reveal the new interactions at the electroweak scale [5–8]. Because of the Glashow-Iliopoulos-Maiani mechanism [9], the SM can only contribute to the top-quark flavor-changing neutral current (FCNC) at loop level with the expected branching ratios around $10^{-15} - 10^{-12}$ [10]. However, such suppression can be relaxed by the extended flavor structures, and consequently larger branching ratios of $t \to qH$ or $t \to qV$ are expected in many new physics (NP) models, for example, in the minimal supersymmetric standard model [11,12], the two-Higgs-doublet models [13,14], extra dimensions [15], little Higgs with T-parity [16] model, and/or the other miscellaneous models [17–19]. So, the measurement of any excess in the branching ratios for top-quark FCNC processes would be an indication to the NP beyond the SM.

At the LHC, top quark can be copiously produced in pair production, which leads to a high precision for the study of top observables, such as its couplings and rare decays [20–31]. On the other hand, the single top and Higgs associated production process $pp \to th$ is also important to search for the FCNC top-Higgs couplings, which has been emphasized in Refs. [32–37]. Up to now, the ATLAS and CMS collaborations have set the upper limits of $\mathrm{Br}(t \to qH) < 0.79\%$ [24] and $\mathrm{Br}(t \to cH) < 0.56\%$ at 95% C.L. [25] using the processes $pp \to t\bar{t} \to Wb + qh \to \ell\nu b + q\gamma\gamma$. The author of Ref. [32] studied the anomalous production of $th$ via the process $pp \to th \to (Wb) + h \to (\ell\nu)b + (b\bar{b})$ at the LHC including complete QCD next-to-leading order (NLO) corrections, where the upper limits on the branching ratios of top-quark rare decays are obtained: $\mathrm{Br}(t \to hu) \leq 4.1 \times 10^{-4}$, $\mathrm{Br}(t \to hc) \leq 1.5 \times 10^{-3}$.

Compared with the top-quark pair production at the LHC, single top production is a very important process because its cross sections are directly proportional to the top's weak couplings. At the LHC, the top quark can be singly produced associated with $W$ bosons ($tW$) via the process $bg \to tW^-$. The cross section is predicted at the NLO plus the contribution due to the resummation of soft-gluon bremsstrahlung [next-to-next-to-leading logarithmic (NNLL)] to be about 41.8 pb at the 14 TeV LHC for $m_t = 173$ GeV [38]. It has been shown that this process is observable at the LHC using the fully simulated data at the CMS and ATLAS detectors [39,40]. Very recently, Ref. [41] has given an experimental review of the study of processes with a single top quark at the LHC, where the $Wtb$ coupling (see, for example, Refs. [42,43]) and other FCNC couplings [44–46] are sensitive to the single top production processes. Although the top pair production process has the largest cross section, other processes with different production mechanisms and final states can also be studied independently and compared with the top-quark pair production. It is therefore worthwhile to perform a complete calculation of the $pp \to W^- t \to W^- hq$ process due to the presence of the top-Higgs FCNC couplings $tqH$. It is a kind of the complementary processes to be studied in addition to the top pair and $th$ production processes.

*liuyaobei@sina.com
†xiaozhenjun@njnu.edu.cn

 

TABLE I. The most stringent upper bounds on the $\mathrm{Br}(t \to qH)$ at 95% C.L. obtained from the ATLAS and CMS collaborations and other phenomenological studies from different channels.

| Limits on branching ratio | Search channel | Data set |
|---|---|---|
| $\mathrm{Br}(t \to qH) < 0.79\%$ | ATLAS $t\bar{t} \to Wb + qH \to \ell\nu b + \gamma\gamma q$ | 4.7, 20 fb$^{-1}$@ 7,8 TeV [24] |
| $\mathrm{Br}(t \to cH) < 0.56\%$ $\mathrm{Br}(t \to uH) < 0.45\%$ | CMS $t\bar{t} \to W^+b + qH \to \ell\nu b + \gamma\gamma q$ | 19.5 fb$^{-1}$@8 TeV [25] |
| $\mathrm{Br}(t \to qH) < 5 \times 10^{-4}$ | ATLAS $t\bar{t} \to W^+b + qH \to \ell\nu b + \gamma\gamma q$ | 3000 fb$^{-1}$@14 TeV [23] |
| $\mathrm{Br}(t \to cH) < 0.19\%$ $\mathrm{Br}(t \to uH) < 0.15\%$ | LHC $th \to \ell^+\nu b + \tau^+\tau^-$ | 100 fb$^{-1}$@13 TeV [33] |
| $\mathrm{Br}(t \to cH) < 0.33\%$ $\mathrm{Br}(t \to uH) < 0.22\%$ | LHC $th \to \ell^+\nu b + \ell^+\ell^- X$ | 100 fb$^{-1}$@13 TeV [33] |
| $\mathrm{Br}(t \to cH) < 0.48\%$ $\mathrm{Br}(t \to uH) < 0.36\%$ | LHC $th \to jjb + b\bar{b}$ | 100 fb$^{-1}$@13 TeV [33] |
| $\mathrm{Br}(t \to cH) < 0.15\%$ $\mathrm{Br}(t \to uH) < 0.041\%$ | LHC $th \to \ell\nu b + b\bar{b}$ at the NLO | 100 fb$^{-1}$@14 TeV [32] |
| $\mathrm{Br}(t \to qH) < 0.12\%$ $\mathrm{Br}(t \to cH) < 0.26\%$ | LHC $t\bar{t} \to W^+b + qH \to \ell^+\nu b + \gamma\gamma q$ | 3000 fb$^{-1}$@14 TeV [27] |
| $\mathrm{Br}(t \to qH) < 0.238\%$ | LHeC $e^-p \to \nu_e\bar{t} \to \nu_e\bar{q}H \to \nu_e\bar{q} + b\bar{b}$ | 100 fb$^{-1}$@150 GeV for $e^-$ [29] |
| $\mathrm{Br}(t \to qH) < 0.112\%$ | ILC $e^+e^- \to t\bar{t} \to tqH \to \ell^+\nu b + b\bar{b}q$ | 3000 fb$^{-1}$@500 GeV [30] |

This paper is arranged as follows. In Sec. II, we briefly describe the top-Higgs FCNC interactions and review the current limits on top-Higgs FCNC processes from direct and indirect searches. In Sec. III, we discuss the observability of the top-Higgs FCNC couplings through the process $pp \to W^-hj$ at 14 TeV LHC. Finally, a short summary is given in Sec. IV.

## II. TOP-HIGGS FCNC COUPLINGS AND CURRENT CONSTRAINTS

Considering the FCNC Yukawa interactions in the framework of the effective field theory, the SM Lagrangian can be extended simply by allowing the terms [47]

$$\mathcal{L} = \lambda_{tuh}\bar{t}Hu + \lambda_{tch}\bar{t}Hc + \mathrm{H.c.}, \tag{1}$$

where the real parameters $\lambda_{tuh}$ and $\lambda_{tch}$ denote the FCNC couplings of $\bar{t}Hu$ and $\bar{t}Hc$. Thus, the total decay width of the top-quark $\Gamma_t$ can be written as the form of

$$\Gamma_t = \Gamma^{\mathrm{SM}}(t \to W^-b) + \Gamma(t \to qH), \tag{2}$$

where $q = u, c$. The decay width of the dominant top-quark decay mode $t \to W^-b$ at the leading order (LO) and the NLO can be found in Ref. [48]. After assuming the dominant top decay width $t \to bW$ and neglecting the up- and charm-quark masses, the branching ratio of $t \to qh$ can be approximately given by the form [33]

$$\begin{aligned}\mathrm{Br}(t \to qh) &= \frac{\lambda_{tqh}^2}{\sqrt{2}m_t^2 G_F}\frac{(1-x_h^2)^2}{(1-x_W^2)^2(1+2x_W^2)}\kappa_{\mathrm{QCD}} \\ &\simeq 0.58\lambda_{tqh}^2,\end{aligned} \tag{3}$$

where $G_F$ is the Fermi constant, $x_W = m_W/m_t$, and $x_h = m_h/m_t$. The factor $\kappa_{\mathrm{QCD}}$ is the NLO QCD correction to $\mathrm{Br}(t \to qh)$, which is calculated as $\kappa_{\mathrm{QCD}} = 1 + 0.97\alpha_s \simeq 1.1$ by the results of high-order corrections to $t \to bW$ [48] and $t \to ch$ [49].

In Table I, we summarize the most stringent upper bounds on the top-Higgs FCNC branching ratios at 95% C.L. obtained from the ATLAS and CMS collaborations and other phenomenological studies from different channels. From Table I, one can see that the stringent constraints of $\mathrm{Br}(t \to cH) < 0.56\%$ and $\mathrm{Br}(t \to uH) < 0.45\%$ were reported by the CMS Collaboration obtained by a combination of the multilepton channel and the diphoton plus lepton channel [25]. Furthermore, the upper limits on the flavor-changing top-quark decays can be significantly improved with the high luminosity. For example, Ref [23] quotes a 95% C.L. limit sensitivity in the $tt \to Wb + hq \to \ell\nu b + \gamma\gamma q$ final state of $\mathrm{Br}(t \to hq) < 5 \times 10^{-4}$ with an integrated luminosity of 3000 fb$^{-1}$ at $\sqrt{s} = 14$ TeV. On the other hand, the low-energy observables, such as $D^0 - \bar{D}^0$ mixing [50] and $Z \to c\bar{c}$ [51], can also be used to constrain the top-quark flavor violation in the $tqH$ vertex. With the 125 GeV Higgs boson mass, upper limits of $\mathrm{Br}(t \to cH) < 2.1 \times 10^{-3}$ have been obtained for the $Z \to c\bar{c}$ decay [30]. Reference [52] derived model-independent constraints on the $tcH$ and $tuH$ couplings that arise from the bounds on hadronic electric dipole moments.

## III. NUMERICAL CALCULATIONS AND DISCUSSIONS

In this section, we search for top-Higgs FCNC couplings through the $pp \to W^-(\to \ell^-\bar{\nu})h(\to \gamma\gamma)j$ channel at the LHC, where $\ell = e, \mu$ and $q = u, c$. The Feynman diagrams are plotted in Figs. 1 and 2 for the partonic processes $bg \to W^-hq$ and $\bar{q}b \to W^-hg$, respectively. In the SM, the $Wh$ + jet production can be seen as part of the inclusive $Wh$ production involving the $WWh$ coupling and the Feynman diagrams, and the related LO and NLO QCD calculations can be found, for example, in Ref. [53].

There are mainly two new kinds of processes that can contribute to the production of $W^-hj$ at the LHC. The first one is the $bg$ fusion process $bg \to W^-hq$, and it is the dominant contribution, as shown in Fig. 1, where $hq$ can be produced not only from an on-shell top quark but also from

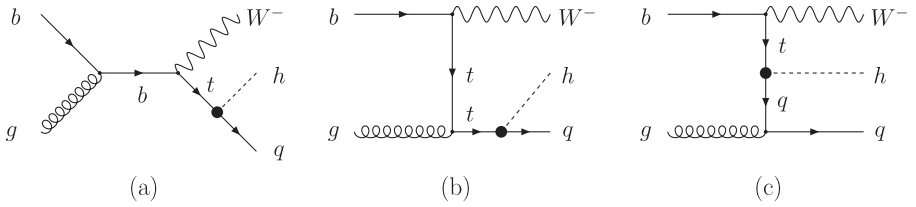


FIG. 1. Feynman diagrams for the partonic process $bg \to W^- hq$ at the LHC through flavor-violating top-Higgs interactions. Here, $q = u, c$.

an off-shell top quark via the new flavor-changing couplings $tqh$. The second one is the $\bar{q}b$ fusion process $\bar{q}b \to W^- hg$, as shown in Fig. 2, which is the subleading contribution. However, such a process is affected by the initial parton distribution functions (PDFs). So, one can use this feature to disentangle the FCNC couplings of the top quark with light quarks. Thus, it is worthwhile to perform a complete calculation of $pp \to W^- hj$ in the presence of the top-Higgs FCNC couplings and explore its sensitivity to probe the top-Higgs FCNC couplings at the LHC experiment.

We first implement the $tqH$ FCNC interactions by using the `FeynRules` package [54] and calculate the LO cross section with `MadGraph5-aMC@NLO` [55]. We use CTEQ6L as the parton distribution function [56] and set the renormalization scale $\mu_R$ and factorization scale $\mu_F$ to be $\mu_R = \mu_F = (m_W + m_h)/2$. In this work, we assume $\lambda_{tqh} \leq 0.1$ to satisfy the direct constraints from the ATLAS and CMS results [24,25]. The SM input parameters are taken as follows [57]:

$$\begin{aligned} m_H &= 125\,\text{GeV}, \quad m_t = 173.21\,\text{GeV}, \\ m_W &= 80.385\,\text{GeV}, \\ \alpha(m_Z) &= 1/127.9, \quad \alpha_s(m_Z) = 0.1185, \\ G_F &= 1.166370 \times 10^{-5}\,\text{GeV}^{-2}. \end{aligned} \tag{4}$$

In Fig. 3, we show the dependence of the cross sections $\sigma_{Whj}$ on the top-Higgs FCNC couplings $\lambda_{tqh}$ at 14 TeV LHC for three different cases: (I) $\lambda_{tqh} = \lambda_{tch}$, $\lambda_{tuh} = 0$, (II) $\lambda_{tqh} = \lambda_{tuh}$, $\lambda_{tch} = 0$, and (III) $\lambda_{tqh} = \lambda_{tuh} = \lambda_{tch}$. Since the analysis does not distinguish between the $t \to ch$ and $t \to uh$ final states which have similar acceptances, we take $\lambda_{tuh} = \lambda_{tch}$ in Case III for the simplicity of calculation. From Fig. 3, one can see that:

(1) For three cases, the dominant contributions to $pp \to W^- hj$ come from the $bg$-fusion process. To be specific, when $\sqrt{s} = 14$ TeV and $\lambda_{tqh} = 0.1$, the full cross sections of $pp \to W^- hj$ are about 1.05, 1.10, and 1.07 times larger than that of $pp \to W^- t \to W^- hq$ in Cases I, II, and III, respectively.

(2) For the same values of $\lambda_{tuh}$ and $\lambda_{tch}$, the cross section of $pp \to W^- hj$ in Case I is smaller to that in Case II, since the charm quark has a smaller PDF than the up quark in the proton. Thus, for a given collider energy and luminosity, we can expect the sensitivity to the coupling $\lambda_{tuh}$ to be better than that to $\lambda_{tch}$.

(3) For $\lambda_{tqh} = 0.1$ in Cases I–III, the total cross sections of $pp \to W^- hj$ are about 158, 162, and 325 fb, respectively, while the cross section for the SM process $pp \to W^- hj$ is about 225 fb with the same input parameters and cuts. Thus, in the following calculations, we will mainly consider the probed sensitivity for Case III due to the relative large cross section.

Although the branching ratio is small, the diphoton decay mode $h \to \gamma\gamma$ of the Higgs boson is one of the two cleanest channels of the Higgs boson, which allows a sharp reconstructed peak right at the Higgs boson mass and has the great advantage that most QCD backgrounds are gone. Thus, in the following calculations, we perform the Monte Carlo simulation and explore the sensitivity of 14 TeV LHC to the top-Higgs FCNC couplings $\lambda_{tqh}$ through the channel,

$$pp \to W^-(\to \ell^- \bar{\nu}_\ell) h(\to \gamma\gamma) j. \tag{5}$$

As can be seen, in this case, the studied topology of our signal gives rise to the jet $+ \not{E}_T +$ diphoton signature

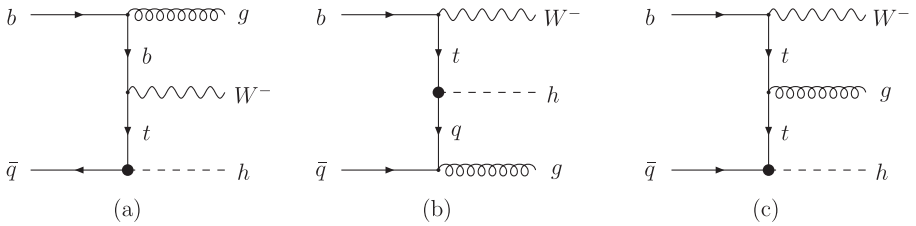


FIG. 2. Feynman diagrams for the partonic process $\bar{q}b \to W^- hg$ at the LHC through flavor-violating top-Higgs interactions. Here, $q = u, c$.

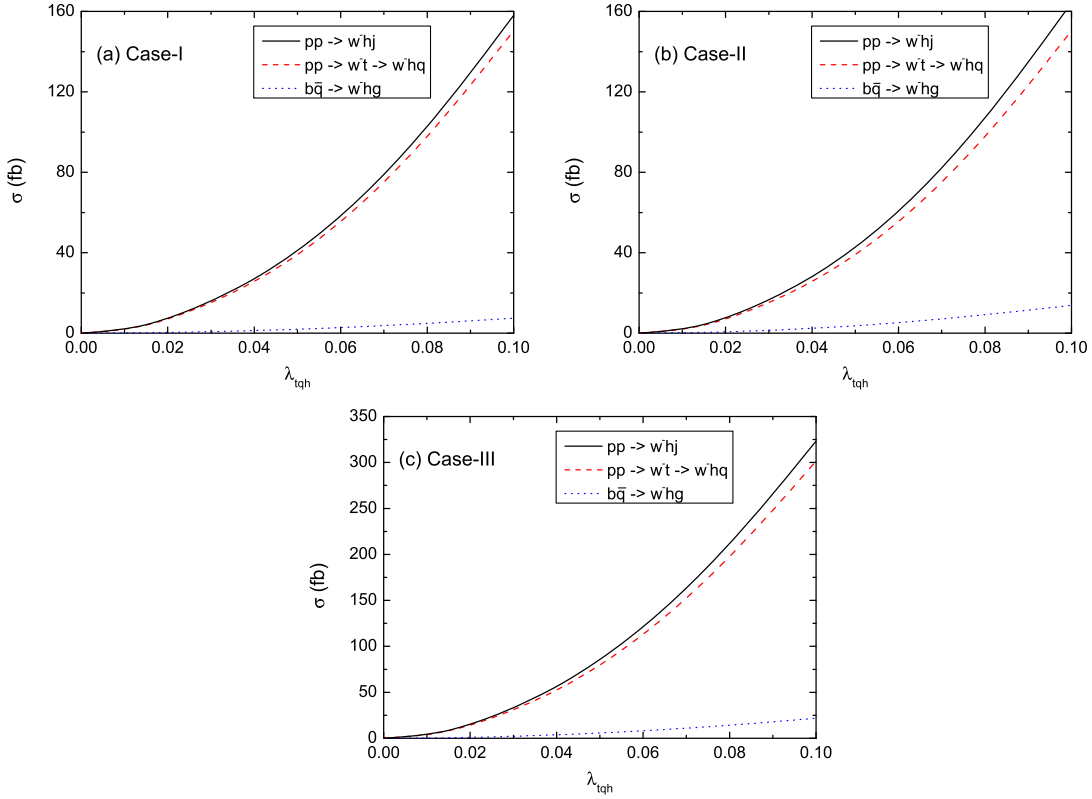


FIG. 3. The dependence of the cross sections $\sigma$ at 14 TeV LHC on the top-Higgs FCNC couplings $\lambda_{tqh}$ for Case I to Case III.

characterized by one jet, one lepton, a missing $\not{E}_T$ from the undetected neutrino, and a diphoton signal appearing as a narrow resonance centered around the Higgs boson mass. The main SM backgrounds which yield the identical final states to the signal include two parts: the resonant and the nonresonant backgrounds. For the former, they mainly come from the processes that have a Higgs boson decaying to a diphoton in the final states, such as $W^-hj$, $Zhj$, and $W^+W^-h$ productions ($j$ denotes non-bottom-quark jets), with one daughter lepton of $Z$ and one of the jets of $W^+$ being mistagged. For the latter, the main background processes contain the diphoton events associatedly produced, such as $W^-j\gamma\gamma$, $Zj\gamma\gamma$, and $\bar{t}j\gamma\gamma$, where $W^-j\gamma\gamma$ is the most dominant background.

All of these signal and backgrounds events are generated at leading order using `MadGraph5 -aMC@NLO`. `PYTHIA` [58] is utilized for parton shower and hadronization. `Delphes` [59] is then employed to account for the detector simulations, and `MadAnalysis5` is used [60] for analysis, where the (mis)tagging efficiencies and fake rates are assumed to be their default values. When generating the parton level events, we assume $\mu_R = \mu_F$ to be the default event-by-event value. The anti-$k_t$ algorithm [61] with the jet radius of 0.4 is used to reconstruct jets. The QCD corrections for the dominant backgrounds are considered by including a $k$ factor, which is 1.12 for $W^-hj$ [53], 1.2 for $Zhj$ [62], and 1.3 for $W^-j\gamma\gamma$ [63,64]. On the other hand, the MLM scheme [65] is used to match our matrix element with a parton shower. Here, it should be mentioned that the $k$ factor for the LO cross section of $\sigma_{tW^-}$ is chosen as 1.53 for the prediction at NLO + NNLL QCD corrections to $tW^-$ production at the 14 TeV LHC [38,66]. Because of the small contribution from the process $b\bar{q} \to W^-hg$, it is safe to take the LO cross section for this subleading process.

In our simulation, we generate 400,000 events for the signals and 400,000 events for the backgrounds. We first employ some basic cuts for the selection of events,

$$p_T^j > 25\ \text{GeV}, \qquad \text{P}_T^\ell > 20\ \text{GeV},$$
$$|\eta_\text{j}| < 2.5, \qquad |\eta_\ell| < 2.0, \qquad \Delta\text{R}_\text{ij} > 0.4, \qquad (6)$$

where $p_T^{j,\ell}$ and $|\eta_{j,\ell}|$ are the transverse momentum and the pseudorapidity of the jet and leptons, respectively. $\Delta R = \sqrt{(\Delta\phi)^2 + (\Delta\eta)^2}$ is the particle separation among the objects (the jet, the lepton, and the photons) in the final state with $\Delta\phi$ and $\Delta\eta$ being the separation in the azimuth angle and rapidity, respectively.

In Fig. 4, we show the distributions of some kinematical variables for the signal (with the fixed parameter $\lambda_{tqh} = 0.1$ in Case III) and backgrounds at 14 TeV LHC. The result of $W^+W^-h$ is not shown since it is subdominant with a very small cross section (at the level of $10^{-3}$ fb) for the same

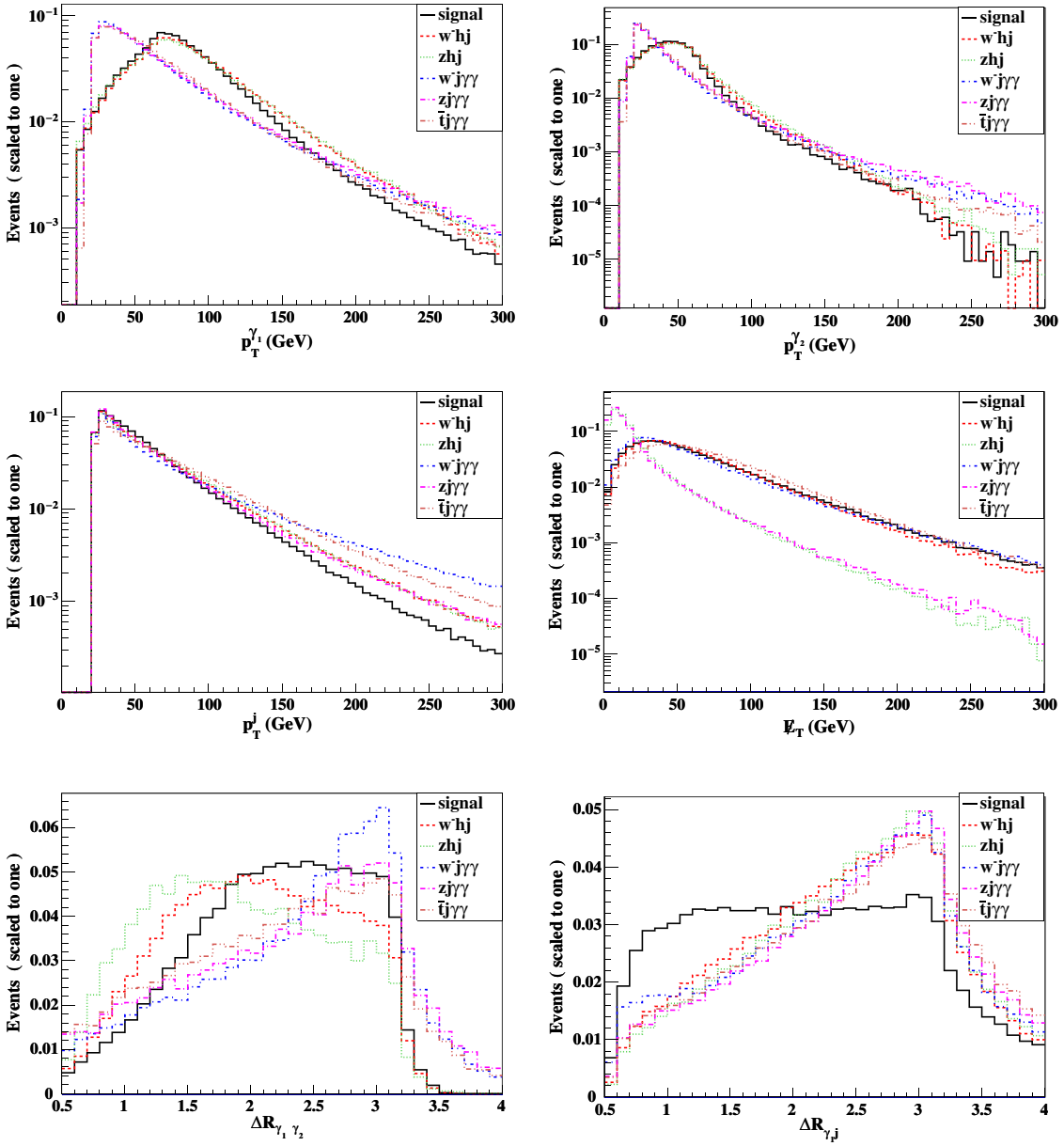


FIG. 4. Normalized distributions of transverse momentum $p_T^{\gamma_1}$, $p_T^{\gamma_2}$, $p_T^{j}$; the transverse missing energy $\not{E}_T$; and various separations $\Delta R_{\gamma_1\gamma_2,\gamma_1 j}$ in the signals and backgrounds at 14 TeV LHC.

final states. According to the distribution differences between the signal and backgrounds, we can improve the ratio of signal to backgrounds by making suitable kinematical cuts. First, since the two photons in the signal and the resonant backgrounds come from the Higgs boson, they have peaks around $m_h/2$ and possess the harder $p_T$ spectrum than those in the nonresonant backgrounds. The distributions of the transverse momentum $p_T^j$ of the jet share a similar feature. The missing transverse energy $\not{E}_T$ in the backgrounds $Zhj$ and $Zh\gamma\gamma$ has a peak at about 10 GeV, while the other share a similar feature, and thus the suitable cut on $\not{E}_T$ can largely suppress these two backgrounds. Thus, we can apply the following cuts to suppress the backgrounds:

$$p_T^{\gamma 1} > 55\ \text{GeV}, \qquad \text{p}_\text{T}^{\gamma 2} > 35\ \text{GeV},$$
$$\text{p}_\text{T}^{\text{j}} < 80\ \text{GeV}, \qquad \not{E}_\text{T} > 20\ \text{GeV}. \tag{7}$$

Second, since two photons in the signals are from the Higgs boson decay, the signal rates peak at their invariant mass around the Higgs mass with relative small separation. The same features are shared by the separation $\Delta R_{\gamma_1 j}$ for the signal and the background, since the jet and the photon in the signal come from the same particle (top quark). These differences between the signal and backgrounds suggest the following comprehensive cuts:

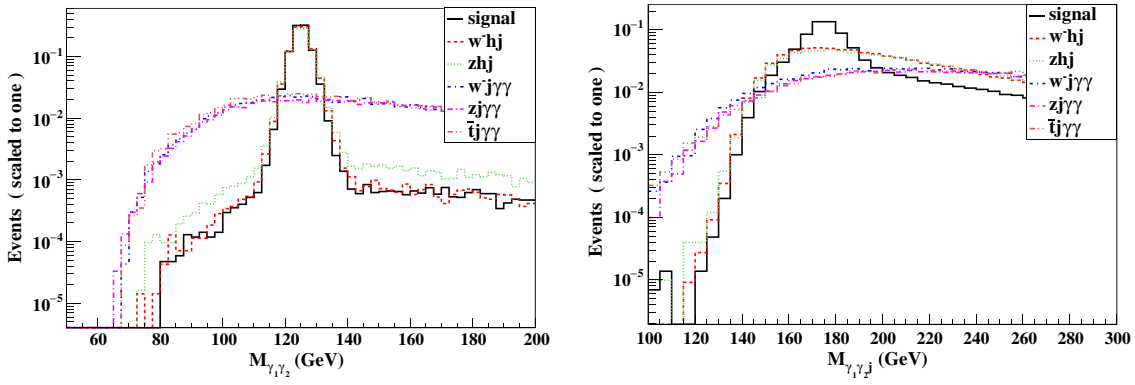


FIG. 5. Normalized invariant-mass distribution of two photons (left) and the diphoton and light jet system (right) at the 14 TeV LHC.

$$1 < \Delta R_{\gamma_1\gamma_2} < 2.7, \qquad 0.5 < \Delta R_{\gamma_1 j} < 2.2. \tag{8}$$

Next, we consider utilizing the invariant-mass distributions to further suppress the background. Figure 5 shows the normalized invariant-mass distribution $M_{\gamma\gamma}$ of two photons and $M_{\gamma\gamma j}$ of the diphoton and light jet system, respectively. Although the diphoton decay channel has a small branching ratio, it has the advantage of good resolution on the $\gamma\gamma$ resonance and is also free from the large QCD backgrounds. Thus, we can use a narrow invariant-mass window $|M_{\gamma\gamma} - m_H| < 5$ GeV to further reduce the nonresonant backgrounds. Very similar to $M_{\gamma\gamma}$, the invariant mass distribution of the diphoton and the light jet $M_{\gamma_1\gamma_2 j}$ also has a peak around the top-quark mass in the signal other than the backgrounds, which can be used to further remove the backgrounds. We therefore impose a cut on $M_{\gamma\gamma j}$:

$$|M_{\gamma\gamma j} - m_t| < 10 \text{ GeV}. \tag{9}$$

For a short summary, we list all the cut-based selections here:

(1) Basic cut: $p_T^j > 25$ GeV, $p_T^\ell > 20$ GeV, $|\eta_j| < 2.5$, $|\eta_\ell| < 2$, and $\Delta R_{ij} > 0.4$ $(i, j = \ell, j, \gamma)$;
(2) Cut 1 means the basic cuts plus missing $\not{E}_T > 20$ GeV, $p_T^{\gamma 1} > 55$ GeV, $p_T^{\gamma 2} > 35$ GeV, and $p_T^j < 80$ GeV;
(3) Cut 2 means Cut 1 plus $1 < \Delta R_{\gamma_1\gamma_2} < 2.7$ and $0.5 < \Delta R_{\gamma_1\gamma_2} < 2.2$;
(4) Cut 3 means Cut 2 plus requiring the invariant mass of the diphoton pair to be in the range $m_h \pm 5$ GeV;
(5) Cut 4 means Cut 3 plus requiring the invariant mass of the diphoton and light jet system to lie in the range $m_t \pm 10$ GeV.

The cross sections of the signal and backgrounds after imposing the cuts are summarized in Table II. For the numbers of the cross sections as listed in Table II, the QCD corrections to the signal and backgrounds are included by a multiplicative $k$ factor of 1.53, 1.12, 1.2, and 1.3 to the leading-order cross sections of $tW^-$ [38,66], $W^-hj$ [53], $Zhj$ [62], and $W^-j\gamma\gamma$ [63,64] at the 14 TeV LHC. In the last column of Table II, we show the signal-to-background ratio $S/B$. From the numerical results as listed in the last line of Table II, one can see that the $W^-hj$ and $W^-j\gamma\gamma$ are two major backgrounds after applying all those mentioned cuts. About 11 signal events can survive after the cuts at the LHC with an integrated luminosity of 1000 fb$^{-1}$ with a signal-to-background ratio of 4.55. We do not consider here the Cases I and II due to their relatively small production rates.

To estimate the observability quantitatively, we adopt the significance measurement [67]

$$SS = \sqrt{2L\left[(S+B)\ln\left(1+\frac{S}{B}\right) - S\right]}, \tag{10}$$

TABLE II. The cut flow of the cross sections (in $10^{-3}$ fb) for the signal ($W^-hq$) in Case III and backgrounds ($W^-hj$, $Zhj$, $W^-j\gamma\gamma$, $Zj\gamma\gamma$, and $\bar{t}j\gamma\gamma$) at the 14 TeV LHC. As a comparison, the corresponding results of the resonant production $pp \to W^-t \to W^-hq$ are also listed in the brackets.

| Cuts | Signal | $W^-hj$ | $Zhj$ | $W^-j\gamma\gamma$ | $Zj\gamma\gamma$ | $\bar{t}j\gamma\gamma$ | $S/B$ |
|---|---|---|---|---|---|---|---|
| Basic cuts | 103 (96.1) | 31.7 | 18.6 | 4268 | 1943 | 195 | 0.016 (0.015) |
| Cut 1 | 25.8 (24.16) | 6.3 | 5.6 | 256 | 33 | 17.5 | 0.081 (0.076) |
| Cut 2 | 15.1 (13.99) | 2.1 | 0.19 | 54.2 | 7.4 | 6.3 | 0.21 (0.19) |
| Cut 3 | 13.23 (12.46) | 1.87 | 0.15 | 3.8 | 0.52 | 0.5 | 1.93 (1.82) |
| Cut 4 | 11.36 (10.71) | 0.63 | 0.066 | 1.36 | 0.2 | 0.24 | 4.55 (4.29) |

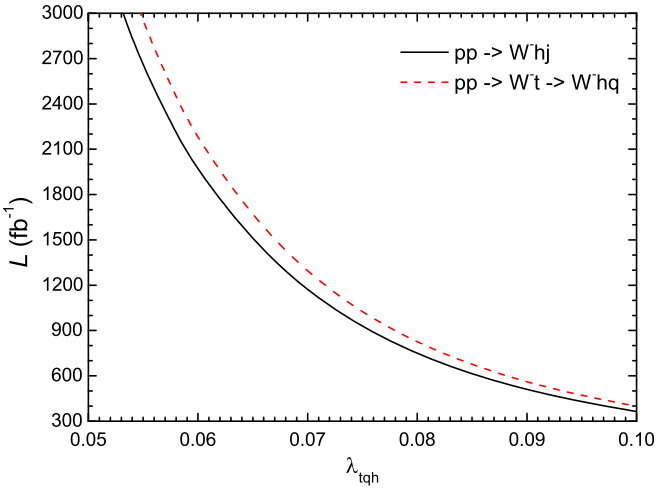


FIG. 6. Contour plots in the $L - \lambda_{tqh}$ plane for $3\sigma$ significance of $pp \to W^- hj$ (solid line) and the resonant production $pp \to W^- t \to W^- hq$ (dashed line) at 14 TeV LHC.

where $S$ and $B$ are the signal and background cross sections and $L$ is the integrated luminosity. In Fig. 6, we plot the contours of $3\sigma$ significance of $pp \to W^- hj$ at 14 TeV LHC for Case III in the plane of $L - \lambda_{tqh}$. From Fig. 6, one can see that the flavor-changing couplings $\lambda_{tqh}$ can be probed to 0.053 at $3\sigma$ statistical sensitivity, which corresponds to the branching ratios $\mathrm{Br}(t \to qh) = 0.16\%$ at 14 TeV LHC with $L = 3000$ fb$^{-1}$. Besides, the corresponding results of the resonant production $pp \to W^- t \to W^- hq$ are also displayed. We can see that the LHC sensitivity to the coupling $\lambda_{tqh}$ from the full calculation of $W^- hj$ production can be improved by about 6% as a compared with the resonant production $pp \to W^- t \to W^- hq$.

In comparison with the direct collider limits as presented in Table I, one can see that our results are similar to those of other studies as given in Refs. [27–30], where the sensitivity bounds of $10^{-3}$ order are obtained through different search channels. For example, Ref. [27] obtained the sensitivity bound of about 0.1–0.3% through the $pp \to t(\to \ell^+ \nu_\ell b) h(\to \gamma\gamma) j$ channels at the 14 TeV with an integrated luminosity of 3000 fb$^{-1}$. However, the production mechanism of our search in this paper is different from the one in Ref. [27], in which the authors mainly consider the top-quark pair production at the LHC via the strong interaction, through processes such as $gg, q\bar{q} \to t\bar{t} \to \ell^+ \nu_\ell b + \bar{q} H$. We expect here to provide the complementary information for detecting the top-Higgs FCNC couplings via the possible but different production processes at the future high-luminosity LHC. In addition, utilizing a more powerful tool, such as the multivariate technique [68] and various decay modes from the Higgs boson, may provide better sensitivity to separate signal from background, as shown in the very recent work [29].

## IV. CONCLUSION

In this paper, we investigated the process $pp \to W^- hj$ induced by the top-Higgs FCNC couplings at the LHC. We found that the cross section of $pp \to W^- hj$ mainly comes from the resonant process $pp \to W^- t \to W^- hq$ due to the anomalous $tqH$ couplings (where $q$ denotes up and charm quarks). We further studied the observability of top-Higgs FCNC couplings through the process $pp \to W^-(\to \ell^- \bar{\nu}_\ell) h(\to \gamma\gamma) j$ and found that the branching ratios $\mathrm{Br}(t \to qh)$ can be probed to 0.16% at $3\sigma$ level at 14 TeV LHC with $L = 3000$ fb$^{-1}$. Compared with the resonant production $pp \to W^- t \to W^- hq$, such a full calculation can increase the LHC $3\sigma$ sensitivity to $\mathrm{Br}(t \to qh)$ by about 6% at 14 TeV LHC with $L = 3000$ fb$^{-1}$ because of the contribution of the nonresonant production $\bar{q}b \to W^- hg$.

## ACKNOWLEDGMENTS

Yao-Bei Liu thanks Zhi-Long Han and Lei Wu for useful discussions about the MadGraph and MadAnalysis5 packages. This work is supported by the National Natural Science Foundation of China under Grant No. 11235005 and the Joint Funds of the National Natural Science Foundation of China (Grant No. U1304112).

[1] G. Aad *et al.* (ATLAS Collaboration), Phys. Lett. B **716**, 1 (2012).
[2] S. Chatrchyan *et al.* (CMS Collaboration), Phys. Lett. B **716**, 30 (2012).
[3] G. Aad *et al.* (ATLAS Collaboration), Phys. Lett. B **726**, 88 (2013).
[4] V. Khachatryan *et al.* (CMS Collaboration), Eur. Phys. J. C **75**, 212 (2015); V. Khachatryan *et al.* (CMS Collaboration) Eur. Phys. J. C**75**, 251 (2015).
[5] C. S. Li, H. T. Li, and D. Y. Shao, Chin. Sci. Bull. **59**, 3709 (2014); C. Zhang and S. Willenbrock, Phys. Rev. D **83**, 034006 (2011); Nuovo Cimento Soc. Ital. Fis. **033**, 285 (2010); W. Bernreuther, J. Phys. G **35**, 083001 (2008); J. A. Aguilar-Saavedra, Nucl. Phys. **B812**, 181 (2009); **B821**, 215 (2009).
[6] E. W. N. Glover *et al.*, Acta Phys. Pol. B **35**, 2671 (2004); D. Chakraborty, J. Konigsberg, and D. L. Rainwater, Annu. Rev. Nucl. Part. Sci. **53**, 301 (2003); M. Beneke *et al.*, arXiv:hep-ph/0003033; T. Han, Int. J. Mod. Phys. A **23**, 4107 (2008).
[7] T. M. P. Tait and C.-P. Yuan, Phys. Rev. D **63**, 014018 (2000); F. Maltoni, K. Paul, T. Stelzer, and S. Willenbrock,

Phys. Rev. D **64**, 094023 (2001); M. Farina, C. Grojean, F. Maltoni, E. Salvioni, and A. Thamm, J. High Energy Phys. 05 (2013) 022; C. Englert and E. Re, Phys. Rev. D **89**, 073020 (2014); J. Ellis, D. S. Hwang, K. Sakurai, and M. Takeuchi, J. High Energy Phys. 04 (2014) 004; S. Biswas, E. Gabrielli, and B. Mele, J. High Energy Phys. 01 (2013) 088; S. Biswas, E. Gabrielli, F. Margaroli, and B. Mele, J. High Energy Phys. 07 (2013) 073.

[8] J. Chang, K. Cheung, J. S. Lee, and C.-T. Lu, J. High Energy Phys. 05 (2014) 062; A. Kobakhidze, L. Wu, and J. Yue, J. High Energy Phys. 10 (2014) 100; Y.-C. Guo, C.-X. Yue, and S. Yang, arXiv:1603.00604.

[9] S. L. Glashow, J. Iliopoulos, and L. Maiani, Phys. Rev. D **2**, 1285 (1970).

[10] G. Eilam, J. L. Hewett, and A. Soni, Phys. Rev. D **44**, 1473 (1991); B. Mele, S. Petrarca, and A. Soddu, Phys. Lett. B **435**, 401 (1998); A. Cordero-Cid, J. M. Hernández, G. Tavares-Velasco, and J. J. Toscano, Phys. Rev. D **73**, 094005 (2006); G. Eilam, M. Frank, and I. Turan, Phys. Rev. D **73**, 053011 (2006); J. A. Aguilar-Saavedra, Acta Phys. Pol. B **35**, 2695 (2004).

[11] J. J. Cao, G. Eilam, M. Frank, K. Hikasa, G. L. Liu, I. Turan, and J. M. Yang, Phys. Rev. D **75**, 075021 (2007); J. Cao, C. Han, L. Wu, J. M. Yang, and M. Zhang, Eur. Phys. J. C **74**, 3058 (2014); T.-J. Gao, T.-F. Feng, F. Sun, H.-B. Zhang, and S.-M. Zhao, Chin. Phys. C **39**, 073101 (2015); S. Bejar, J. Guasch, D. Lopez-Val, and J. Sola, Phys. Lett. B **668**, 364 (2008); M. Frank and I. Turan, Phys. Rev. D **74**, 073014 (2006); S. Bejar, J. Guasch, and J. Sola, J. High Energy Phys. 10 (2005) 113; J. L. Diaz-Cruz, H.-J. He, and C.-P. YuanPhys. Lett. B **530**, 179 (2002); J. Guasch and J. Sola, Nucl. Phys. **B562**, 3 (1999); C. S. Li, R. J. Oakes, and J. M. Yang, Phys. Rev. D **49**, 293 (1994) **56**, 3156 (1997); J. M. Yang and C. S. Li, Phys. Rev. D **49**, 3412 (1994).

[12] Z.-X. Heng, G.-R. Lu, L. Wu, and J. M. Yang, Phys. Rev. D **79**, 094029 (2009); J. Cao, Z. Heng, L. Wu, and J. M. Yang, Phys. Rev. D **79**, 054003 (2009); J. M. Yang, B.-L. Young, and X. Zhang, Phys. Rev. D **58**, 055001 (1998); G. Eilam, A. Gemintern, T. Han, J. M. Yang, and X. Zhang, Phys. Lett. B **510**, 227 (2001); M. Frank and I. Turan, Phys. Rev. D **72**, 035008 (2005).

[13] T. Han and R. Ruiz, Phys. Rev. D **89**, 074045 (2014); K.-F. Chen, W.-S. Hou, C. Kao, and M. Kohda, Phys. Lett. B **725**, 378 (2013); C. Kao, H.-Y. Cheng, W.-S. Hou, and J. Sayre, Phys. Lett. B **716**, 225 (2012); A. Arhrib, K. Cheung, C. W. Chiang, and T. C. Yuan, Phys. Rev. D **73**, 075015 (2006); E. O. Iltan and I. TuranPhys. Rev. D **67**, 015004 (2003); S. Bejar, J. Guasch, and J. Sola, Nucl. Phys. **B600**, 21 (2001); S. Bar-Shalom, G. Eilam, A. Soni, and J. Wudka, Phys. Rev. Lett. **79**, 1217 (1997); W. S. Hou, G.-L. Lin, and C.-Y. Ma, Phys. Rev. D **56**, 7434 (1997); J. L. Diaz-Cruz, R. Martinez, M. A Perez, and A. Rosado, Phys. Rev. D **41**, 891 (1990).

[14] D. Atwood, L. Reina, and A. Soni, Phys. Rev. D **55**, 3156 (1997); R. Gaitan, R. Martinez, and J. H. M. de Oca, arXiv:1503.04391; G. Abbas, A. Celis, X. Q. Li, J. Lu, and A. Pich, J. High Energy Phys. 06 (2015) 005; B. Altunkaynak, W. S. Hou, C. Kao, M. Kohda, and B. McCoy, Phys. Lett. B **751**, 135 (2015).

[15] K. Agashe, G. Perez, and A. Soni, Phys. Rev. D **75**, 015002 (2007).

[16] B. Yang, N. Liu, and J. Han, Phys. Rev. D **89**, 034020 (2014).

[17] F. del Aguila, J. A. Aguilar-Saavedra, and R. Miquel, Phys. Rev. Lett. **82**, 1628 (1999); J. A. Aguilar-Saavedra and B. M. Nobre, Phys. Lett. B **553**, 251 (2003); J. Cao, K. Hikasa, L. Wang, L. Wu, and J. M. Yang, Phys. Rev. D **85**, 014025 (2012).

[18] C.-X. Yue, S.-Y. Cao, and Q.-G. Zeng, J. High Energy Phys. 04 (2014) 170; C. Han, N. Liu, L. Wu, and J. M. Yang, Phys. Lett. B **714**, 295 (2012); J. Cao, L. Wu, and J. M. Yang, Phys. Rev. D **83**, 034024 (2011); G.-R. Lu and L. Wu, Chin. Phys. Lett. **27**, 031401 (2010); J. Drobnak, S. Fajfer, and J. F. Kamenik, J. High Energy Phys. 03 (2009) 077; J. Cao, Z. Xiong, and J. M. Yang, Nucl. Phys. **B651**, 87 (2003).

[19] A. Azatov, G. Panico, G. Perez, and Y. Soreq, J. High Energy Phys. 12 (2014) 082; J. Cao, L. Wang, L. Wu, and J. M. Yang, Phys. Rev. D **84**, 074001 (2011); J. Cao, Z. Heng, L. Wu, and J. M. Yang, Phys. Rev. D **81**, 014016 (2010); A. Azatov, M. Toharia, and L. Zhu, Phys. Rev. D **80**, 035016 (2009); K. Agashe and R. Contino, Phys. Rev. D **80**, 075016 (2009).

[20] P. M. Ferreira, R. B. Guedes, and R. Santos, Phys. Rev. D **77**, 114008 (2008); F. Larios, R. Martinez, and M. A. Perez, Int. J. Mod. Phys. A **21**, 3473 (2006); J. M. Yang, Ann. Phys. (Amsterdam) **316**, 529 (2005);

[21] N. Craig, J. A. Evans, R. Gray, M. Park, S. Somalwar, S. Thomas, and M. Walker, Phys. Rev. D **86**, 075002 (2012).

[22] E. Yazgan (ATLAS, CDF, CMS, and D0 Collaborations), arXiv:1312.5435.

[23] ATLAS Collaboration, ATL-PHYS-PUB-2013-012.

[24] G. Aad *et al.* (ATLAS Collaboration), J. High Energy Phys. 06 (2014) 008.

[25] (CMS Collaboration), CMS-PAS-HIG-13-034, 2014.

[26] K. Agashe *et al.* (Top Quark Working Group Collaboration), arXiv:1311.2028.

[27] Lei Wu, J. High Energy Phys. 02 (2015) 061.

[28] W. Liu, H. Sun, X. Wang, and X. Luo, Phys. Rev. D **92**, 074015 (2015).

[29] H. Sun, arXiv:1602.04670.

[30] H. Hesari, H. Khanpour, and M. M. Najafabadi, Phys. Rev. D **92**, 113012 (2015).

[31] G. Aad *et al.* (ATLAS Collaboration), J. High Energy Phys. 12 (2015) 061.

[32] Y. Wang, F. P. Huang, C. S. Li, B. H. Li, D. Y. Shao, and J. Wang, Phys. Rev. D **86**, 094014 (2012).

[33] A. Greljo, J. F. Kamenik, and J. Kopp, J. High Energy Phys. 07 (2014) 046.

[34] S. Khatibi and M. M. Najafabadi, Phys. Rev. D **89**, 054011 (2014).

[35] D. Atwood, S. K. Gupta, and A. Soni, J. High Energy Phys. 10 (2014) 57.

[36] D. Lopez-Val, J. Guasch, and J. Sola, J. High Energy Phys. 12 (2007) 054.

[37] J. A. Aguilar-Saavedra and G. C. Branco, Phys. Lett. B **495**, 347 (2000).

[38] N. Kidonakis, Phys. Rev. D **82**, 054018 (2010).

[39] G. L. Bayatian *et al.* (CMS Collaboration), J. Phys. G **34**, 995 (2007).

[40] A. Airapetian *et al.* (ATLAS Collaboration), CERN-LHCC-99-15.
[41] A. Giammanco, Rev. Phys. **1**, 1 (2016).
[42] J. M. Yang and B.-L. Young, Phys. Rev. D **56**, 5907 (1997); Z. Lin, T. Han, T. Huang, J. Wang, and X. Zhang, Phys. Rev. D **65**, 014008 (2001); C.-R. Chen, F. Larios, and C.-P. Yuan, Phys. Lett. B **631**, 126 (2005); Q.-H. Cao, J. Wudka, and C.-P. Yuan, Phys. Lett. B **658**, 50 (2007); E. L. Berger, Q.-H. Cao, and I. Low, Phys. Rev. D **80**, 074020 (2009); Q.-H. Cao, B. Yan, J.-H. Yu, and C. Zhang, arXiv:1504.03785.
[43] P. Batra and T. M. Tait, Phys. Rev. D **74**, 054021 (2006); C. Zhang and S. Willenbrock, Phys. Rev. D **83**, 034006 (2011); G. Durieux, F. Maltoni, and C. Zhang, Phys. Rev. D **91**, 074017 (2015).
[44] G. Aad *et al.* (ATLAS Collaboration), Phys. Lett. B **712**, 351 (2012); Eur. Phys. J. C **76**, 55 (2016).
[45] V. Khachatryan *et al.* (CMS Collaboration), J. High Energy Phys. 04 (2016) 035.
[46] S. M. Etesami and M. M. Najafabadi, Phys. Rev. D **81**, 117502 (2010).
[47] C. Degrande, J.-M. Gerard, C. Grojean, F. Maltoni, and G. Servant, Phys. Lett. B **703**, 306 (2011).
[48] C. S. Li, R. J. Oakes, and T. C. Yuan, Phys. Rev. D **43**, 3759 (1991).
[49] C. Zhang and F. Maltoni, Phys. Rev. D **88**, 054005 (2013); J. Drobnak, S. Fajfer, and J. F. Kamenik, Phys. Rev. Lett. **104**, 252001 (2010); J. J. Zhang, C. S. Li, J. Gao, H. Zhang, Z. Li, C.-P. Yuan, and T.-C. Yuan, Phys. Rev. Lett. **102**, 072001 (2009); C. Zhang and F. Maltoni, Phys. Rev. D **88**, 054005 (2013).
[50] J. I. Aranda, A. Cordero-Cid, F. Ramírez-Zavaleta, J. J. Toscano, and E. S. Tututi, Phys. Rev. D **81**, 077701 (2010).
[51] F. Larios, R. Martinez, and M. A. Perez, Phys. Rev. D **72**, 057504 (2005).
[52] M. Gorbahn and U. Haisch, J. High Energy Phys. 06 (2014) 033.
[53] J. J. Su, W.-G. Ma, R.-Y. Zhang, and L. Guo, Phys. Rev. D **81**, 114037 (2010).
[54] A. Alloul, N. D. Christensen, C. Degrande, C. Duhr, and B. Fuks, Comput. Phys. Commun. **185**, 2250 (2014).
[55] J. Alwall, M. Herquet, F. Maltoni, O. Mattelaer, and T. Stelzer, J. High Energy Phys. 06 (2011) 128; 07 (2014) 079.
[56] J. Pumplin, A. Belyaev, J. Huston, D. Stump, and W. K. Tung, J. High Energy Phys. 02 (2006) 032.
[57] K. A. Olive *et al.* (Particle Data Group Collaboration), Chin. Phys. C **38**, 090001 (2014).
[58] T. Sjostrand, S. Mrenna, and P. Z. Skands, J. High Energy Phys. 05 (2006) 026.
[59] J. de Favereau, C. Delaere, P. Demin, A. Giammanco, V. Lemaître, A. Mertens, and M. Selvaggi (DELPHES 3 Collaboration), J. High Energy Phys. 02 (2014) 057.
[60] E. Conte, B. Fuks, and G. Serret, Comput. Phys. Commun. **184**, 222 (2013).
[61] M. Cacciari, G. P. Salam, and G. Soyez, J. High Energy Phys. 04 (2008) 063.
[62] J. J. Su, L. Guo, W.-G. Ma, R.-Y. Zhang, L.-S. Ling, and L. Han, J. High Energy Phys. 03 (2012) 059.
[63] F. Campanario, C. Englert, M. Rauch, and D. Zeppenfeld, Phys. Lett. B **704**, 515 (2011).
[64] J. Alwall, R. Frederix, S. Frixione, V. Hirschi, F. Maltoni, O. Mattelaer, H.-S. Shao, T. Stelzer, P. Torrielli, and M. Zaro, J. High Energy Phys. 07 (2014) 079.
[65] R. Frederix and S. Frixione, J. High Energy Phys. 12 (2012) 061.
[66] S. Zhu, Phys. Lett. B **524**, 283 (2002); **537**, 351(E) (2002)].
[67] G. Cowan, K. Cranmer, E. Gross, and O. Vitells, Eur. Phys. J. C **71**, 1554 (2011).
[68] A. Hoecker *et al.*, *Proc. Sci.*, ACAT2007 (2007) 040; CERN-OPEN-2007-007.